Robust PCA-Based Dimensionality Reduction in Human Hand Coordination

Cahree Myrick, Ramana Vinjamuri, and Rajasekhar Anguluri

***Abstract*— We consider robust principal component analysis (RPCA) to perform dimensionality reduction for human hand motor control based on kinematic synergies. RPCA decomposes joint angular velocity data into (i) a low-rank matrix capturing coordinated motion patterns and (ii) a sparse matrix isolating sensor artifacts. Next we apply a robust LASSO method to find synergy recruitment weights, yielding a sparse representation of hand grasping tasks. Experiments on 100 grasp trials show that RPCA maintains stable performance up to approximately 20% corruption, while classical PCA degrades quickly. Our results suggest that robustifying standard PCA and LASSO enables reliable synergy extraction even with inexpensive, low-quality sensors, supporting affordable experimentation and improved prosthetic or robotic hand control.**

Keywords: PCA, Robust PCA, Kinematic Synergies, Robust LASSO, Hand Coordination.

I. Introduction

Recent research has demonstrated the advantage of modeling complex human hand movements as linear combinations of a few kinematic synergies [1]–[4]. This modeling paradigm has paved the way for many dimensionality reduction methods to extract these latent synergies from angular velocity data of specific finger joints. A comprehensive evaluation of the performance of different linear and nonlinear reduction methods is provided in [5].

Principal Component Analysis (PCA) is widely used to extract synergies from hand movement, with LASSO [6] subsequently applied to determine optimal weights for combining these synergies to reconstruct hand velocities. LASSO stands for Least Absolute Shrinkage and Selection Operator and refers to the ℓ_1-norm regularized least squares problem; see Section III. This two-step approach is popular due to its simplicity and interpretability.

However, neither PCA nor LASSO is robust to extreme data deviations, including outliers or missing values (occlusions) [7], [8]. These issues often arise in hand movement experiments like grasping tasks due to sensing limitations. High-resolution camera systems like Vicon, widely used in research, suffer from joint occlusions, while instrumented devices like the CyberGlove, which measure joint angles via embedded sensors, often experience signal loss. Both approaches are thus prone to data deviations.

To address these challenges, we propose using robust variants of PCA and LASSO to improve synergy extraction and velocity reconstruction for hand movements. By handling outliers and occlusions effectively, our methods enable more accurate modeling of hand kinematics.

The first author is a junior student in the Department of Mathematics and the last two authors are affliated with the Department of Computer Science and Electrical Engineering, University of Maryland, Baltimore County, MD 85281, USA ((e-mail:{cmyrick1,rvinjam1,rajangul}@umbc.edu).

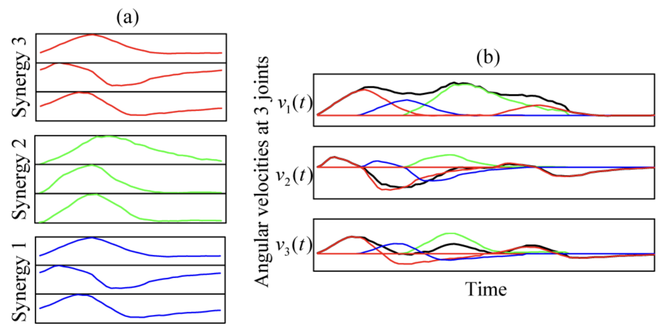

Fig. 1: Three synergies, each repeated three times in (a), combine to produce hand velocities (in black) at all joints in (b). Reproduced from [2].

II. Research Question

Let $v_i(t)$ be the angular velocity of the ith hand joint at time t and define the vector $\mathbf{v}(t) = [v_1(t), \dots, v_n(t)]^\top$ of angular velocities, corresponding to the n joints of the hand at t. Then $\mathbf{v}(t)$ obeys the convolution-mixture model [2]:

$$\mathbf{v}(t) = \sum_{j=1}^{m} \sum_{k=1}^{K_j} c_{jk}\, \mathbf{s}_j\big(t - t_{jk}\big) + \mathbf{e}(t), \tag{1}$$

where $\mathbf{s}_j(t) = [s_{1j}(t), \dots, s_{nj}(t)]^\top$ is the kinematic synergy vector with $j \in \{1, \dots, m\}$, and m denotes the total number of synergies; K_j accounts for the number of repeats (recruitments) of the j-th synergy; the scalars c_{jk} are non-negative amplitudes; and t_{jk} represent time shifts. In Fig. 1, we have $m = 3$ and $n = 3$. The outer summation indexes the m synergies, while the inner summation allows for multiple repeats of each synergy. For instance, in Fig. 1, the first synergy is activated twice. Finally, the vector $\mathbf{e}(t)$ accounts for outliers or occlusions and is discussed in Section IV.

Problem: Develop a numerical method to find the smallest number of synergies m, the fewest activations K_j per synergy, and to recover the corresponding synergy waveforms $\mathbf{s}_j$ and weights c_{jk} in (1), given velocity data $\mathbf{v}(t)$ corrupted by sparse outliers ($\mathbf{e}(t)$ has more zeros than non-zeros).

III. Methods

A direct approach to our problem is to jointly solve for c_{jk} and $\mathbf{s}_j$ by formulating an optimization (e.g., least-squares). However, the resulting problem is non-convex, often yielding suboptimal solutions. Importantly, iterative algorithms used to solve such problems are computationally expensive; see

[9] for further discussion. An alternative two-stage approach [2] is to first extract synergies from a set of *training data*, followed by estimation of c_{jk} using separate *test data*.

A. PCA plus LASSO approach ([2] no outliers/missing data)

Let $\mathbf{e}(t) = 0$. We construct the angular-velocity matrix V from training data comprising angular velocities of joints recorded during rapid-grasping tasks. Let $v_i^g(t)$ denote the velocity of joint $i \in \{1, \ldots, n\}$ at time t (with $t = 1, \ldots, T$) during the gth task (with $g = 1, \ldots, G$). Then,

$$V = \begin{bmatrix} v_1^1(1) & \cdots & v_1^1(T) & \cdots & v_n^1(1) & \cdots & v_n^1(T) \\ \vdots & \vdots & \vdots & \ddots & \vdots & \vdots & \vdots \\ v_1^g(1) & \cdots & v_1^g(T) & \cdots & v_n^g(1) & \cdots & v_n^g(T) \\ \vdots & \vdots & \vdots & \ddots & \vdots & \vdots & \vdots \\ v_1^G(1) & \cdots & v_1^G(T) & \cdots & v_n^G(1) & \cdots & v_n^G(T) \end{bmatrix} \tag{4}$$

contains G rows and Tn columns. Each row corresponds to one grasping task having velocities of all n joints over time.

The smallest set of synergies is extracted from the right singular vectors of the optimal low-rank approximation of V. Let the SVD of V be $V = U\Sigma S$. The desired synergy matrix S_m is given by the top m rows of S and m is the target low-rank dimension. Each row of the matrix S_m represents a synergy waveform of all joints. A PCA-based justification for this SVD approach is in [2], [5].

The second stage involves using S_m as an estimate for the synergy waveforms $\mathbf{s}_j$ in (1) and subsequently solving for the optimal coefficients c_{jk}. This allows us to reconstruct velocities using the mixture model in (1). To this aim, one constructs an overcomplete matrix B, composed of time-shifted versions of the synergies in S_m; see [2, Section II.C]. By straightforward algebraic manipulation of terms in (1), we can rewrite the mixture-model compactly as

$$\mathbf{v}_{\text{test}}^\top = \mathbf{c}^\top B, \tag{2}$$

where $\mathbf{c}^\top$ is the row vector containing c_{jk}, and the row vector $\mathbf{v}_{\text{test}}^\top = \begin{bmatrix} v_1^1(1) & \cdots & v_1^1(T_t) | & \cdots & | v_n^1(1) & \cdots & v_n^1(T_t) \end{bmatrix}$ corresponds to a single grasping task. Here, $T_t \neq T$ denotes the duration of the task in the testing phase. By stacking $\mathbf{v}_{\text{test}}^\top$ on top of each other we get a matrix similar to (4).

Since our overall goal of dimensionality reduction is to use the smallest number of synergies with the few recruitments, we estimate the optimal sparse vector $\mathbf{c}$ in (2) by solving the following LASSO minimization problem:

$$\min_{\mathbf{c}} \quad \|\mathbf{v}_{\text{test}} - B\mathbf{c}\|_2^2 + \lambda\|\mathbf{c}\|_1. \tag{3}$$

Here, the tuning parameter $\lambda > 0$ controls the sparsity level of $\mathbf{c}$; the ℓ_1-norm $\|\mathbf{c}\|_1$ denotes the sum of the absolute values of the entries in $\mathbf{c}$; and $\|\mathbf{x}\|_2^2$ denotes the sum of the squares of the entries in $\mathbf{x}$ for some arbitrary vector $\mathbf{x}$.

B. RPCA plus RLASSO approach

The PCA-plus-LASSO approach is theoretically valid only when $\mathbf{e}(t) = 0$, or when $\mathbf{e}(t)$ follows a normal distribution with small variance. However, in the presence of outliers or missing data (i.e., when $\mathbf{e}(t) \neq 0$ exhibits gross corruption), this approach breaks down. To address this challenge, we propose robust variants to both PCA and LASSO that are resilient to such data imperfections.

Let $\tilde{V} = V + E$, where V is in (4), and E is a sparse outlier matrix that shares the same structure as V but contains mostly zeros, with a few large-magnitude nonzero entries. RPCA estimates a low-rank approximation of V by solving the following convex optimization problem [8]:

$$\min_{V,E} \; \|V\|_* + \lambda\,\|E\|_1 \quad \text{s.t. } \tilde{V} = V + E, \tag{4}$$

where the nuclear norm $\|\cdot\|_*$ promotes low rank (i.e., fewer synergies) and the ℓ_1-norm $\|\cdot\|_1$ helps isolate outliers. From the optimal low-rank V recovered via RPCA, we extract the synergy matrix S_m using the procedure discussed earlier.

To recover the sparse coefficients c_{jk} in (1), we construct the overcomplete matrix B using the synergies extracted from RPCA. We then model the test data in the presence of outliers as $\tilde{\mathbf{v}}_{\text{test}}^\top = \mathbf{c}^\top B + \mathbf{e}^\top$. Robust LASSO (RLASSO) then estimates the optimal sparse coefficients by solving the following regularized minimization problem:

$$\min_{\mathbf{c},\,\mathbf{e}} \quad \|\mathbf{v}_{\text{test}} - B\mathbf{c}\|_2^2 + \lambda_1\|\mathbf{c}\|_1 + \lambda_2\|\mathbf{e}\|_1, \tag{5}$$

where $\lambda_1, \lambda_2 > 0$ promote sparsity in the coefficients $\mathbf{c}$ and in the outlier term $\mathbf{e}$, respectively.

The solutions to the optimization problems in (3), (4), and (5) do not admit closed-form formulas, and are solved using iterative algorithms. We implemented these methods using standard off-the-shelf Python packages [10].

C. Grasping Task Reconstruction Error

To quantify the accuracy of the two approaches discussed above, we compute the squared distance error between the true velocity profile for a given grasping task, often $\mathbf{v}_{\text{test}}$, and its estimate $\hat{\mathbf{v}} = B\hat{\mathbf{c}}$, where $\hat{\mathbf{c}}$ is obtained as the minimizer of either (3) or (5). The cumulative error is thus given by

$$\text{Error} = \frac{1}{G}\sum_{g=1}^{G} \left\| \mathbf{v}_{\text{true}}^{(g)} - \hat{\mathbf{v}}^{(g)} \right\|_2^2,$$

where G is the total number of grasping tasks. We then average this error across all subjects and report the resulting value as a function of the percentage outliers or missing data.

IV. SIMULATIONS

We used proprietary data from prior experiments described in [2]. A right-handed CyberGlove with 22 joint-angle sensors was employed, of which 10 (thumb MCP/IP and finger MCP/PIP joints) were analyzed during grasping tasks by ten subjects. From this velocity data, we constructed the clean matrix V in (4) and the testing data vector $\mathbf{v}_{\text{test}}$ in (2).

We refer readers to [2] for descriptions of the experimental setup used to obtain the clean training data matrix V in (4) and the testing data vector $\mathbf{v}_{\text{test}}$ in (2). The parameters are as

TABLE I: RPCA versus PCA (no. of synergies)

Corruption (%)	*joint_dropout*		*time_local_mild*		*time_local_severe*	
	PCA	RPCA	PCA	RPCA	PCA	RPCA
0%	6	4	6	4	6	4
5%	7	4	7	4	6	4
10%	8	4	8	4	7	5
15%	10	5	10	4	8	5
20%	10	7	11	4	8	6

follows: $n = 10$ joints; training data duration $T = 39$; testing data duration $T_t = 82$; and total number of grasping tasks $G = 100$. Thus, V is a 100×390 matrix, and $\mathbf{v}_{\text{test}}^\top$ is a row vector of dimension $nT_t = 820$. Note that we constructed these velocity matrices for a total of 10 subjects.

The matrix B has 820 rows and mK columns, where K denotes the number of time shifts and m is determined based on the approximation accuracy index:

$$\frac{\lambda_1^2 + \ldots + \lambda_m^2}{\lambda_1^2 + \ldots + \lambda_{100}^2},$$

where λ_i are the singular values of V in (4) for PCA, while for RPCA the singular values are obtained from the low-rank minimizer in (4). This index quantifies the percentage the total variance (due to grasping tasks) explained by the top m synergies. A larger index indicates a better approximation of the (velocity) data by the selected synergies. We set 95% as the standard threshold to determine m [11].

A. Dataset Preparation

(Case 1: Sensor Dropout Outliers) In instrumented gloves like the CyberGlove, signal loss from strain gauge or flex sensors can cause sudden slips or jerks. We simulate outliers by adding large-magnitudes at randomly chosen times in V. Formally, for the g-th row of $\tilde{V}$, corresponding to the g-th grasping task, the g-th row of E contains $\rho\%$ nonzero entries selected uniformly at random, representing the outliers. Here, ρ ranges from 0 to 20. Each nonzero entry is generated by adding a spike drawn uniformly between 2× and 4× the true measurement magnitude.

(Case 2: Occlusion Outliers) They occur in optical systems when joints are invisible to cameras due to occlusion (e.g., overlapping limbs). In the data matrix V, these appear as contiguous blocks of zeroed out samples. Each row of V, $\rho\%$ of its entries are zeroed out as follows: (i) *joint_dropout:* 1–2 occlusion blocks having 8–15 samples each, restricted to one joint; (ii) *time_local_mild:* 1–3 occlusion blocks with 5–10 samples per block; and (iii) *time_local_severe:* 4–8 large occlusion blocks with 20–40 samples per block. Note that (ii) and (iii) can span multiple joints.

Note that PCA+LASSO and RPCA+RLASSO are implemented on corrupted data, even though PCA+LASSO is developed for clean data in [2]. This enables a quantitative comparison of its performance relative to robust methods.

B. Synergy Extraction Results

These results highlight the robustness of RPCA for synergy extraction in the presence of data corruption. We first present the synergy extraction results for both the outlier and occlusion datasets. Figure 2 shows the number of principal components (or synergies) required by RPCA and PCA to capture at least 95% of the variance in the data matrix as the percentage of sparse outlier corruption increases. RPCA consistently achieves this target with only $m = 4$ synergies, even at a corruption level of 20%, whereas the number of synergies required by standard PCA increases sharply. This behavior is expected, as RPCA effectively separates genuine hand dynamics from sparse outliers, preserving a fixed low-dimensional synergy subspace, while PCA treats the outliers as part of the signal and consequently introduces additional synergies as corruption increases.

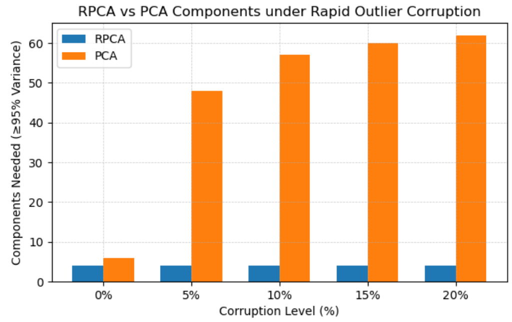

Fig. 2: Number of PCs (synergies) required to explain 95% of the variance (in the V matrix) vs. rapid-outlier corruption level. Results are averaged across 10 subjects.

TABLE II: RPCA versus PCA (synergy similarity)

Corruption (%)	directional alignment			vector difference		
	PC1	PC2	PC3	PC1	PC2	PC3
0%	0.9997	0.9877	-0.9760	0.0235	0.1361	1.9870
5%	0.9937	0.9548	-0.8670	0.1112	0.2961	1.2816
10%	0.9895	0.9327	-0.7616	1.0679	0.3609	1.3771
15%	0.9830	0.8672	-0.4661	1.0822	0.6893	1.2974
20%	0.9782	0.7944	-0.2538	0.2083	0.6407	1.5834

Table I highlights the advantage of RPCA over PCA when dealing with structured block occlusions. Across all conditions (*joint_dropout*, *time_local_mild*, and *time_local_severe*), we observe that the number of synergies required to explain 95% of the data variance rises as the corruption percentage rises. However, this increase is gradual for RPCA, whereas for PCA, even a corruption as low as 10% results in a substantial increase in the number of synergies.

Table II presents two similarity metrics comparing PCA and RPCA synergies as the corruption percentage increases. We evaluate (i) *directional alignment*, computed using the dot product between matched synergies of PCA and RPCA (capturing directional similarity, including polarity), and (ii) *vector discrepancy*, defined as the $\|\cdot\|_2$-norm difference between corresponding synergies (capturing shape mismatch). Both metrics are averaged across subjects.

For the first synergy or principal component (PC1), directional alignment drops slightly from 0.9997 at 0% corruption to 0.9782 at 20%, while discrepancy remains low, indicating

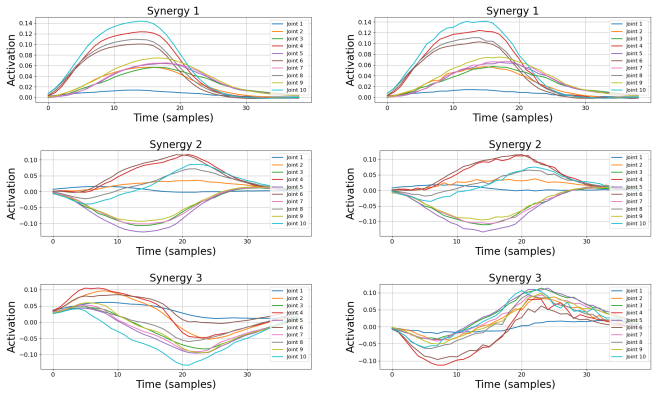

Fig. 3: First three (dominant) kinematic synergies obtained for subject 1 using clean data via PCA (left) and 15% data corrupted with rapid-outliers (right) via RPCA. The number of time samples is 39.

TABLE III: Average Reconstruction Error (rapid-outliers)

Corruption (%)	LASSO mean (std)	RLASSO mean (std)
0%	0.263 (0.065)	0.253 (0.066)
5%	0.272 (0.074)	0.257 (0.072)
10%	0.284 (0.080)	0.258 (0.070)
15%	0.296 (0.085)	0.263 (0.069)
20%	0.305 (0.088)	0.263 (0.068)

negligible distortion. Instead, PC2 exhibits greater sensitivity to corruption: alignment decreases from 0.9877 to 0.7944, indicating gradual misalignment, and discrepancy rises moderately from 0.1361 to 0.6407.

Our results show that higher-order synergies (e.g., PC3) degrade most under sparse outliers, with directional alignment dropping from -0.9760 to -0.2538 and vector discrepancy remaining above 1.2. In contrast, PC1, which captures dominant variance, remains robust even at 20% corruption, demonstrating RPCA's effectiveness in preserving low-rank structure. Finally, to assess structural stability, Fig. 3 displays the first three synergies extracted by PCA and RPCA at 0% and 15% rapid-outlier corruption for a single subject.

C. *Grasping Task Reconstruction*

Tables III and IV report averaged mean-squared velocity reconstruction error for rapid-outliers and occlusion settings, respectively. In fact, from Table III, we see that RLASSO maintains a stable error profile (0.253 to 0.263) as corruption increases from 0% to 20%, whereas standard LASSO exhibits a steady rise in the reconstruction error (0.263 to 0.305). Similarly, Table IV demonstrates that across all three occlusion types, RLASSO consistently achieves lower reconstruction error than LASSO. While LASSO errors gradually increase with occlusion severity and corruption level (for e.g., from 0.263 to 0.292) under joint dropout), RLASSO shows more stability (e.g., 0.253 to 0.277 in the same case).

In summary, our results highlight the robustness of the RPCA+RLASSO framework, which not only preserves accuracy under structured occlusion but also suppresses the impact of missing data better than standard PCA+LASSO.

TABLE IV: Average Reconstruction Error (block occlusion)

Corruption (%)	*joint-dropout*		*time-local-mild*	
	LASSO	RLASSO	LASSO	RLASSO
0%	0.263 (0.065)	0.253 (0.066)	0.263 (0.065)	0.253 (0.066)
5%	0.270 (0.070)	0.256 (0.067)	0.269 (0.068)	0.255 (0.066)
10%	0.278 (0.073)	0.258 (0.066)	0.276 (0.071)	0.259 (0.067)
15%	0.285 (0.075)	0.267 (0.071)	0.283 (0.074)	0.263 (0.068)
20%	0.292 (0.074)	0.277 (0.073)	0.289 (0.073)	0.268 (0.067)
Corruption (%)	*time-local-severe*			
	LASSO	RLASSO		
0%	0.263 (0.065)	0.253 (0.066)		
5%	0.269 (0.069)	0.256 (0.068)		
10%	0.276 (0.070)	0.260 (0.067)		
15%	0.281 (0.071)	0.267 (0.070)		
20%	0.289 (0.072)	0.279 (0.072)		

V. Conclusion

We applied RPCA to extract synergies from rapid hand grasping movements corrupted by rapid outliers (due to sudden signal loss) and data occlusions (where joint movements are invisible to cameras). We then used these synergies to reconstruct hand movements using a RLASSO approach. Comparing these robust methods with standard PCA and LASSO techniques, our results show that the robust methods achieve better dimensionality reduction and comparable reconstruction errors. Further, the directional alignment and vector discrepancy metrics further reveal how the synergies extracted by RPCA differ from those obtained via PCA. Overall, although robust methods require more sophisticated iterative algorithms, they offer a strong alternative for handling data with a significant percentage outliers.

References

[1] Marco Santello, Martha Flanders, and John F Soechting. Postural hand synergies for tool use. *J. of neuroscience*, 18(23):10105–10115, 1998.

[2] Ramana Vinjamuri, Mingui Sun, Cheng-Chun Chang, Heung-No Lee, Robert J Sclabassi, and Zhi-Hong Mao. Dimensionality reduction in control and coordination of the human hand. *IEEE transactions on biomedical engineering*, 57(2):284–295, 2009.

[3] Andrea d'Avella and Emilio Bizzi. Shared and specific muscle synergies in natural motor behaviors. *Proceedings of the national academy of sciences*, 102(8):3076–3081, 2005.

[4] Bo Huang, Caihua Xiong, Wenbin Chen, Jiejunyi Liang, Bai-Yang Sun, and Xuan Gong. Common kinematic synergies of various human locomotor behaviours. *Royal Society open science*, 8(4):210161, 2021.

[5] Ramana Vinjamuri, Wei Wang, Mingui Sun, and Zhi-Hong Mao. Application of linear and nonlinear dimensionality reduction methods. In *Principal Component Analysis*. IntechOpen, 2012.

[6] Robert Tibshirani. Regression shrinkage and selection via the lasso. *Journal of the Royal Statistical Society Series B: Statistical Methodology*, 58(1):267–288, 1996.

[7] Huan Xu, Constantine Caramanis, and Shie Mannor. Robust regression and lasso. *NeurIPS*, 21, 2008.

[8] Emmanuel J Candès, Xiaodong Li, Yi Ma, and John Wright. Robust principal component analysis? *Journal of the ACM*, 58(3):1–37, 2011.

[9] Ramana Vinjamuri, Zhi-Hong Mao, Robert Sclabassi, and Mingui Sun. Time-varying synergies in velocity profiles of finger joints of the hand during reach and grasp. In *IEEE Engineering in Medicine and Biology Society*, pages 4846–4849. IEEE, 2007.

[10] Daniel Foreman-Mackey. pcp: Principal component pursuit in python. https://github.com/dfm/pcp, 2015.

[11] Ian T Jolliffe and Jorge Cadima. Principal component analysis: a review and recent developments. *Philosophical transactions of the royal society A: Mathematical, Physical and Engineering Sciences*, 374(2065):20150202, 2016.